Journal of Materials Chemistry C

Accepted Manuscript

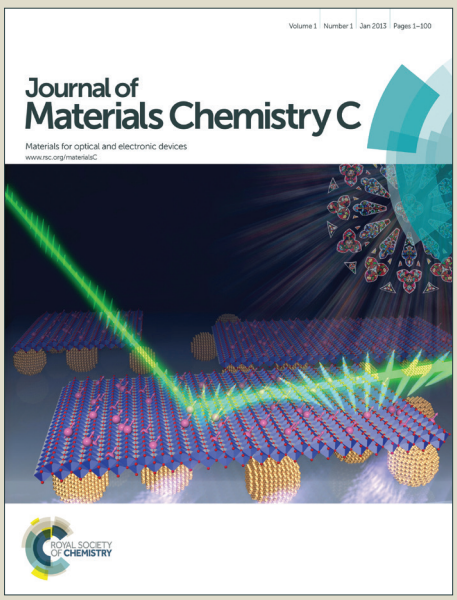

ROYAL SOCIETY OF CHEMISTRY

www.rsc.org/materialsC

Cite this: DOI: 10.1039/c0xx00000x

www.rsc.org/xxxxxx

ARTICLE TYPE

Preparation and Ion Recognition Features of Porphyrin-chalcone Type Compounds as efficient Red-fluorescent Materials

Nuno M. M. Moura,[a,b,c] Cristina Núñez,[*b,d,e] M. Amparo F. Faustino,[a] José A. S. Cavaleiro,[a] M. Graça P. M. S. Neves,[*a] José Luis Capelo,[b,c] Carlos Lodeiro[*b,c]

Received (in XXX, XXX) Xth XXXXXXXXX 20XX, Accepted Xth XXXXXXXXX 20XX
DOI: 10.1039/b000000x

A series of porphyrins containing an α,β-unsaturated ketone unit in a β-pyrrolic position (**4a-e**) were synthesized and characterized. Their sensing ability towards Ag^{+}, Cu^{2+}, Zn^{2+}, Cd^{2+}, $Hg^{2+}$was evaluated in solution by absorption and fluorescence spectroscopy and in gas phase using MALDI-TOF-MS spectrometry. The versatility of this type of compounds towards other metals was also analysed by studying the behaviour of compound **4d** in the presence of Na^{+}, K^{+}, Tl^{+}, Ca^{2+}, Mg^{2+}, Mn^{2+}, Co^{2+}, Ni^{2+}, Pb^{2+}, Fe^{2+}, Fe^{3+}, Cr^{3+} and Al^{3+}. Polymeric films of polymethylmethacrylate (PMMA) doped with ligand **4d** were prepared and their ability to be used as metal ion-probes in the solid state was studied. Compounds of type **4** showed the best performance to be analytically used in developing new Zn^{2+} ratiometric molecular devices.

Introduction

A great interest of the scientific community in the recognition and in the sensing of biological and environmental important metal ions has emerged as a significant goal in the last years.[1-8]

In this field a special attention has been given to fluorescent molecular probes due to the properties inherent to the associated fluorescence technique - simplicity, quickness, high detection limit, it is non-destructive and can be used in bio-imaging.[1,9-12]

In fact, the detection and quantification of trace metal ions with a selective fluorescent reagent has become an important topic of research and are responsible by the remarkable development on this type of probes. These compounds must show stability, high metal affinity, efficient signal transduction, fluorescent signalling, kinetically rapid sensitization and availability.[13]

Porphyrins and related macrocycles are considered to exhibit suitable properties to be used as fluorescent probes namely large Stokes shifts and relatively long excitation (>400 nm) and emission (>600 nm) wavelengths.[14,15] Most of the studies reported in the literature are based on porphyrinic derivatives functionalized in *meso* positions and the results demonstrated their high potential for the detection of metal ions such as Zn^{2+}, Cd^{2+} or Hg^{2+}.[14-20]

The interest in the detection of metals such as zinc(II) is related with its abundance and biological role in mammals.[21] This metal is involved in brain activity, gene transcription, immune function and mammalian reproduction but also in some pathological processes, such as Alzheimer´s disease, epilepsy, ischemic stroke and infantile diarrhea.[22-24] The detection and the determination of trace amounts of heavy metals like mercury(II) or cadmium(II) are also a subject of great concern due to their non-biodegradability and extremely toxic impact on the environment and human health. These highly pollutant metal ions can accumulate in organs and induce disorders such as renal and central nervous system dysfunction or cancer.[16,25] Therefore, the development of new and more efficient probes for detection and determination of trace amounts of heavy and transition metal ions is a subject of great actuality.

Carbon-carbon bond formation *via* aldol type condensation is a powerful tool in organic synthesis and has been extensively studied in the synthesis of α,β-unsaturated ketones like chalcones.[26-28] Recently and concerning our interest in β-functionalization of *meso*-tetraarylporphyrins[29] we described an easy synthetic approach to new benzoporphyrins **1a-e** and porphyrin-2-ylpyridines **2a-e** (Figure 1) through aldol type condensation and Kröhnke type reaction. The procedure involves the reaction of 2-formyl-5,10,15,20-tetraphenylporphyrin **3** with the adequate aryl methyl ketone in refluxing toluene in the presence of catalytic amounts of $La(OTf)_3$ and using ammonium acetate as base.[30] In that work we observed in some experiments the formation of porphyrin-chalcone type derivatives and we had mechanistic evidence that they are the key intermediates in the formation of compounds **1** and **2,** isolated as the major products under those conditions. Since chalcone derivatives find applications in several areas, namely in medicine,[31-34] in the development of optical materials[35-37] or as building blocks in organic synthesis,[38,39] we decided to reevaluate the reactional conditions in order to obtain in those condensations the porphyrin-chalcones type derivatives (**4a-e**, Scheme 1) as the main products.

Taking into account that the presence of the extra chain in the porphyrin core could improve the sensorial ability of these series of compounds and considering our research interest on

the development of fluorescent and colorimetric probes,[40-45] we studied the sensorial ability of these new porphyrins containing the unsaturated unit in the *β*-pyrrolic position (**4a-e**) by spectrophotometric and spectrofluorimetric titrations towards the metal ions Ag^{+}, Cu^{2+}, Zn^{2+}, Cd^{2+}, Hg^{2+}. Based on the results obtained, the versatility of this type of compounds was evaluated by studying the sensorial ability of compound **4d** towards other metals like Na^{+}, K^{+}, Tl^{+}, Ca^{2+}, Mg^{2+}, Mn^{2+}, Co^{2+}, Ni^{2+}, Pb^{2+}, Fe^{2+}, Fe^{3+}, Cr^{3+} and Al^{3+}. The ability of the novel ligands to act as probes in the solid state was also investigated by preparing PMMA films doped with ligand **4d**, and in the gas phase by using MALDI-TOF-MS spectrometry.

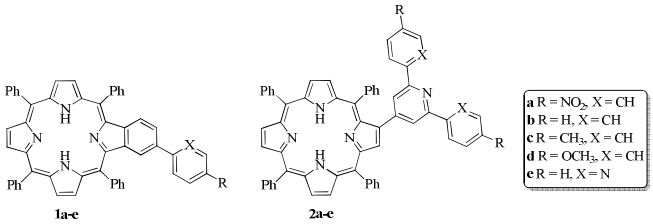

Fig. 1 Structures of benzoporphyrins (**1a-e**) and porphyrin-2-ylpyridines (**2a-e**) derivatives.

EXPERIMENTAL SECTION

General Remarks

Melting points were measured on a Buchi Melting Point B-540 apparatus. ^{1}H and ^{13}C solution NMR spectra were recorded on Bruker Avance 300 (300.13 and 75.47 MHz, respectively) spectrometer. $CDCl_3$ was used as solvent and tetramethylsilane (TMS) as internal reference; the chemical shifts are expressed in δ (ppm) and the coupling constants (*J*) in Hertz (Hz).

Unequivocal ^{1}H assignments were made using 2D COSY ($^{1}H/^{1}H$), while ^{13}C assignments were made on the basis of 2D HSQC ($^{1}H/^{13}C$) and HMBC (delay for long-range *J* C/H couplings were optimized for 7 Hz) experiments. Infra-red spectra were measured with a Perkin-Elmer Paragon 1000 model.

Mass spectra were recorded using MALDI TOF/TOF 4800 Analyzer, Applied Biosystems MDS Sciex, with $CHCl_3$ as solvent and without matrix. Mass spectra HRMS were recorded on APEXQe FT-ICR (BrukerDaltonics, Billerica, MA) mass spectrometer-using $CHCl_3$ as solvent; in *m/z* (rel. %). The UV-Vis spectra were recorded on an UV-2501 PC Shimadzu spectrophotometer using $CHCl_3$ as solvent. Preparative thin-layer chromatography was carried out on 20×20 cm glass plates coated with silica gel (0.5 mm thick). Column chromatography was carried out using silica gel (Merck, 35-70 mesh). Analytical TLC was carried out on precoated sheets with silica gel (Merck 60, 0.2 mm thick).

Chemicals and Starting Reagents

$NaBF_4$, KBF_4, $AgBF_4.xH_2O$, $TlNO_3$, $Ca(BF_4)_2.xH_2O$, $Mg(OTf)_2$, $MnCl_2$, $Co(BF_4)_2.6H_2O$, $Ni(BF_4)_2.xH_2O$, $Cu(BF_4)_2.6H_2O$, $Zn(BF_4)_2.xH_2O$, $Zn(NO_3)_2.xH_2O$, $Zn(OTf)_2.xH_2O$, $ZnCl_2$, $Cd(CF_3SO_3)_2.xH_2O$, $Hg(CF_3SO_3)_2.xH_2O$, $Pb(OTf)_2$, $Fe(NO_3)_3.H_2O$, $Fe(Cl_2).xH_2O$, $Cr(NO_3)_3.xH_2O$ and $Al(NO_3)_3.H_2O$ were purchased from Strem Chemicals, Sigma-Aldrich or Solchemar. All these chemicals were used without further purification. The solvents were obtained from Panreac and Riedel-de-Häen and were used as received or distilled and dried using standard procedures according to the literature procedures.[46]

Synthesis of Organic Ligands

Synthesis of the precursor porphyrins

The 2-formyl-5,10,15,20-tetraphenylporphyrin **3** was prepared from 5,10,15,20-tetraphenylporphyrinate copper(II), *N,N´*-dimethylformamide (DMF) and phosphorus oxychloride ($POCl_3$), according to literature procedure.[47]

Synthesis of porphyrin-chalcone type derivatives 4a-e: general procedure

To a solution of the appropriate aryl methyl ketone (1.2 equiv.) in dry toluene (1 mL) was added piperidine (1.5 equiv.) and the mixture was stirred for 30 min. at room temperature. After this time 2-formyl-5,10,15,20-tetraphenylporphyrin **3** and $La(OTf)_3$ (20 mol%) were added to the mixture and it was heated at reflux for 24 h. After cooling, the reaction mixture was washed with water and extracted with chloroform. The organic layer was separated, dried under Na_2SO_4 and the solvent was evaporated under reduced pressure. The crude mixture was purified by column chromatography (silica gel) using toluene/light petroleum (1:1) and toluene as the eluent. The compounds isolated were then crystallized form CH_2Cl_2/hexane and fully characterized by NMR, mass and UV-Vis techniques. The yields are summarized in Scheme 1. The structures of compounds **1a-e** are in accordance with literature[30] and the full characterization of compounds **4a-e** (Scheme 1) is presented below.

2-[3-(4-Nitrophenyl)-3-oxoprop-1-en-1-yl]-5,10,15,20-tetraphenylporphyrin, 4a:
Purple solid. **m.p.**: > 300 ºC. **^{1}H NMR** (300 MHz, $CDCl_3$): δ 9.10 (1H, s, H-3), 8.85 (2H, AB, *J* = 5.1 Hz, H-β), 8.81-8.79 (3H, m, H-β), 8.73 (1H, AB, *J* = 4.8 Hz, H-β). 8.34 (2H, d, *J* = 8.8 Hz, H-3´´,5´´), 8.25-8.17 (6H, m, H-*o*-Ph), 8.08-8.05 (2H, m, H-*o*-Ph), 7.96 (2H, d, *J* = 8.8 Hz, H-2´´,6´´), 7.82-7.74 (9H, m, H-*m,p*-Ph), 7.57-7.55 (3H, m, H-*m,p*-Ph), 7.45 (2H, AB, *J* = 15.6 Hz, H-1´and H-2´), -2.57 (2H, s, N*H*) ppm. **^{13}C NMR** (75 MHz, $CDCl_3$): δ 190.7 (*C*=O), 150.3, 149.6, 143.4, 143.3, 142.0, 141.8, 141.6, 141.5, 134.54, 134.52, 134.2, 133.1-130.0 (C-β), 129.6, 129.0, 128.6, 128.55, 128.50, 128.3, 128.2, 128.1, 127.9, 127.0, 126.84, 126.80, 126.7, 124.1, 123.6, 120.8, 120.5, 120.4, 120.1 ppm. **IR** (KBr) υ_{max}: 3441.37, 3319.20, 3053.01, 3023.14, 2920.44, 2850.13, 2360.07, 1659.64, 1635.42, 1596.25, 1587.26, 1471.72, 1440.62, 1347.05, 1276.82, 1210.69, 1176.37, 1121.18, 1071.52, 964.02, 797.86, 699.32 cm^{-1}. **UV-Vis** ($CHCl_3$): $\lambda_{máx}$ (log ε) 435.0 (5.05), 526.5 (4.07), 570.5 (3.62), 602.0 (3.61), 663.4 (3.30) nm. **MS** (MALDI): *m/z* 790.2 $[M+H]^{+}$. **HRMS-ESI (+)**: *m/z* calcd for $C_{53}H_{36}N_5O_3$ $[M+H]^{+}$ 790.2818; found 790.2798.

2-[3-Oxo-3-phenylprop-1-en-1-yl]-5,10,15,20-tetraphenylporphyrin, 4b:
Purple solid. **m.p.**: 246.0-247.0 ºC. **^{1}H NMR** (300 MHz, $CDCl_3$): δ 9.07 (1H, s, H-3), 8.83 (2H, AB, *J* = 5.1 Hz, H-β)

8.81-8.75 (4H, m, H-β), 8.25-8.17 (6H, m, H-*o*-Ph), 8.10-8.04 (2H, m, H-*o*-Ph), 7.90 (2H, d, *J* = 7.1 Hz, H-2´´,6´´), 7.80-7.73 (9H, m, H-*m,p*-Ph), 7.60-7.58 (4H, m, H-*m,p*-Ph and H-4´´), 7.53-7.46 (4H, m, H-1´, H-2´ and H-3´´,5´´), -2.68 (2H, s, N*H*) ppm. **^{13}C NMR** (75 MHz, $CDCl_3$): δ 191.9 (*C*=O), 142.1, 142.0, 141.7, 141.3, 138.4, 134.6, 134.5, 134.0, 132.2, 129.0, 128.7, 128.4, 128.2, 128.0, 127.8, 127.1, 126.81, 126.80, 126.7, 125.3, 124.8, 120.6, 120.43, 120.38, 120.2 ppm. **IR** (KBr) υ_{max}: 3442.01, 3292.20, 3074.60, 3052.43, 2922.73, 2851.88, 1692.30, 1662.71, 1597.60, 1580.03,1520.32, 1472.52, 1440.24, 1344.10, 1259.50, 1205.17, 1071.84, 1010.86, 963.84, 853.45, 833.55, 801.31, 734.46, 700.10 cm^{-1}.**UV-Vis** ($CHCl_3$): $\lambda_{máx}$ (log ε) 433.4 (5.29), 524.4 (4.24), 562.0 (3.84), 599.4 (3.78), 659.0 (3.52) nm. **MS** (MALDI): *m/z* 745.2 $[M+H]^+$. **HRMS-ESI (+)**: *m/z* calcd for $C_{53}H_{37}N_4O$ $[M+H]^+$ 745.2967; found 745.2953.

2-[3-Oxo-3-(*p*-tolyl)prop-1-en-1-yl]-5,10,15,20-tetraphenylporphyrin, 4c:

Purple solid. **m.p.**: 246.3-247.4 ºC. **^{1}H NMR** (300 MHz, $CDCl_3$): δ 9.06 (1H, s, H-3), 8.83-8.76 (6H, m, H-β), 8.25-8.17 (6H, m, H-*o*-Ph), 8.09-8.06 (2H, m, H-*o*-Ph), 7.85-7.73 (11H, m, H-*m,p*-Ph and H-2´´,6´´), 7.63-7.61 (3H, m, H-*m,p*-Ph), 7.49 (2H, AB, *J* = 15.4 Hz, H-1´and H-2´), 7.30 (2H, d, *J* = 8.1 Hz, H-3´´,5´´), 2.47 (3H, s, CH_3), -2.68 (2H, s, N*H*) ppm. **^{13}C NMR** (75 MHz, $CDCl_3$): δ 191.0 (*C*=O), 143.0, 142.1, 142.0, 141.7, 141.3, 140.7, 135.8, 134.6, 134.5, 134.1, 129.2, 128.9, 128.6, 128.0, 127.8, 127.1, 126.80, 126.76, 126.7, 124.6, 120.5, 120.4, 120.2, 21.7 (*C*H_3) ppm. **IR** (KBr) υ_{max}: 3451.92, 3307.45, 3050.07, 3027.25, 2914.76, 2851.39, 2541.54, 1655.26, 1604.46, 1586.34, 1470.60, 1439.22, 1333.44,1273.08, 1218.41, 1177.15,1113.06, 1070.54, 1014.95, 962.87, 986.76, 974.50, 794.58, 753.93, 726.86, 699.13 cm^{-1}. **UV-Vis** ($CHCl_3$): $\lambda_{máx}$ (log ε) 434.5 (5.22), 524.5 (4.22), 568.0 (3.84), 601.4 (3.78), 660.5 (3.52) nm. **MS** (MALDI): 759.2 $[M+H]^+$. **HRMS-ESI(+)**: *m/z* calcd for $C_{54}H_{39}N_4O$ $[M+H]^+$ 759.3125; found 759.3124.

2-[3-(4-Methoxyphenyl)-3-oxoprop-1-en-1-yl]-5,10,15,20-tetraphenylporphyrin, 4d:

Purple solid. **m.p.**: > 300 ºC. **^{1}H NMR** (300 MHz, $CDCl_3$): δ 9.05 (1H, s, H-3), 8.85-8.76 (6H, m, H-β), 8.25-8.18 (6H, m, H-*o*-Ph), 8.10-8.07 (2H, m, H-*o*-Ph), 7.96 (2H, AB, *J* = 8.9 Hz, H-2´´,6´´), 7.81-7.65 (12H, m, H-*m,p*-Ph), 7.55 and 7.47 (2H, AB, *J* = 15.3 Hz, H-1´and H-2´), 7.00 (2H, AB, *J* = 8.9 Hz, H-3´´,5´´), 3.92 (3H, s, O*C*H_3), -2.59 (2H, s, N*H*) ppm. **^{13}C NMR** (75 MHz, $CDCl_3$): δ 189.5 (*C*=O), 163.1, 142.2, 142.0, 141.7, 141.3, 140.2, 134.6, 134.5, 134.1, 131.6, 131.2, 130.9, 130.2, 129.0, 128.7, 128.2, 128.0, 128.7, 127.1, 126.80, 126.76, 126.7, 124.3, 120.5, 120.4, 120.1, 113.7 (C-3´´,5´´), 55.5 (O*C*H_3) ppm. **IR** (KBr) υ_{max}: 3449.14,3327.40, 3288.51,3054.24, 3022.26,2903.28, 2834.83, 1656.84, 1597.78, 1469.99, 1439.83, 1347.35, 1332.83, 1249.49, 1214.24,1169.24, 1071.77, 1000.97, 963.86, 833.00, 798.79,732.97, 699.26 cm^{-1}. **UV-Vis** ($CHCl_3$): $\lambda_{máx}$ (log ε): 433.5 (5.20), 524.5 (4.19), 567.4 (3.83), 601.4 (3.74), 660.0 (3.45) nm. **MS** (MALDI): *m/z* 775.3 $[M+H]^+$. **HRMS-ESI (+)**: *m/z* calcd for $C_{54}H_{38}N_4O_2$ $[M]^{+\bullet}$ 774.2995; found 774.2988.

2-[3-Oxo-3-(pyridin-2-yl)prop-1-en-1-yl]-5,10,15,20-tetraphenylporphyrin, 4e:

Purple solid. **m.p.**: 270.8-271.6 ºC. **^{1}H NMR** (300 MHz, $CDCl_3$): δ 9.18 (1H, s, H-3), 8.84-8.79 (6H, m, H-β), 8.75 (1H, d, *J* = 4.7 Hz, H-6´´), 8.25-8.13 (9H, m, H-*o*-Ph and H-3´´), 7.89 (1H, dt, *J* = 1.6 and 7.8 Hz, H-4´´), 7.79-7.69 (14H, m, H-*m,p*-Ph, H-1´ and H-2´), 7.49 (1H, ddd, *J* = 1.3, 4.7 and 7.8 Hz, H-5´´), -2.56 (2H, s, N*H*) ppm. **^{13}C NMR** (75 MHz, $CDCl_3$): δ 189.4 (*C*=O), 154.6, 148.7, 142.1, 142.0, 141.7, 141.5, 141.3, 137.0, 134.6, 134.5, 134.3, 131.9-130.5 (C-β), 129.0, 128.7, 128.5, 127.9. 127.8, 127.2, 126.8, 126.7, 126.6, 123.1, 122.4, 120.7, 120.4, 120.3, 120.2 ppm. **IR** (KBr) υ_{max}: 3438.80, 3308.80, 3052.51, 3024.57, 2920.88, 2849.07, 2357.49,1667.20,1592.35, 1578.03, 1471.90, 1440.10, 1336.20, 1220.40,1176.90, 1120.48, 1072.21, 1020.04, 964.06, 798.44, 751.20, 766.84, 726.34, 699.78 cm^{-1}. **UV-Vis** ($CHCl_3$): $\lambda_{máx}$ (log ε) 437.5 (5.05), 525.5 (4.15), 573.0 (3.83), 602.5 (3.74), 662.0 (3.44) nm. **MS** (MALDI): *m/z* 746.2 $[M+H]^+$. **HRMS-ESI(+)**: *m/z* calcd for $C_{52}H_{36}N_5O$ $[M+H]^+$ 746.2920; found 746.2906.

Gas-phase Measurements

The MALDI-MS analyses were performed in a MALDI-TOF-TOF-MS model Ultraflex II (Bruker, Germany) equipped with nitrogen, from the BIOSCOPE group. Each spectrum represents accumulations of 5 x 50 laser shots. The reflection mode was used. The ion source and flight tube pressure were less than 1.80 x 10^{-7} and 5.60 x 10^{-8} Torr, respectively. The MALDI mass spectra of the soluble samples (1 or 2 μg/μL) were recorded using the "dried droplet" and the "layer-by-layer" sample preparation methods. In both methods the ligands were dissolved in chloroform and the metal salts in acetonitrile but the introduction in the sample holder was different. In the "dried-droplet" method, the two solutions containing the ligand (1 μL) and the metal salt (1 μL) were mixed and then applied in the MALDI-TOF-MS sample holder. In the "layer-by-layer" method, a solution of each ligand was spotted in the MALDI-TOF plate and then dried; subsequently, 1 μL of the solution containing the metal salt was placed on the sample holder, which was then inserted in the ion source. In this case, the chemical reaction between the ligand and the metal salts occurred in the holder, and the complex species were produced in gas phase.

Spectrophotometric and Spectrofluorimetric Measurements

Absorption spectra were recorded on a JASCO V-650 spectrophotometer and fluorescence emission spectra were recorded on a Horiba Jobin-Yvon Fluoromax 4 spectrofluorimeter. The linearity of the fluorescence emission *versus* the concentration was checked in the concentration range used (10^{-4}-10^{-6} M). The correction of the absorbed light was performed when it was considered necessary. The spectrophotometric characterizations and titrations were performed by preparing stock solutions of the compounds in chloroform (*ca.* 10^{-3} M) in a 10 mL volumetric flask. The studied solutions were prepared by appropriate dilution of the stock solutions up to 10^{-5}-10^{-6} M. Titrations of the molecular probes **4a-e** were carried out by the addition of microliter amounts of standard solutions of the metal ions in acetonitrile. All the measurements were performed at 298 K.

Fluorescence quantum yields of compounds **4a-e** were measured using a solution of crystal violet in methanol as standard ([Φ] = 0.54),[48,49] and all values were corrected taking in account the solvent refractions index.

Fluorescence spectra of solid samples were recorded using a fiber optic system connected to a Horiba Jobin-Yvon Fluoromax 4 spectrofluorimetric exciting at appropriated λ

(nm) of the solid compounds. The limit of detection (LOD) and the limit of quantification (LOQ) for metal ions were performed having in mind their use for real anion detection and for analytical applications. For these measurements, ten different analyses for the selected receptor were performed in order to obtain the LOQ. The LOD was obtained by the formula:

$$ydl = yblank + 3\ std$$

where ydl = signal detection limit and std = standard deviation.

Preparation of PMMA polymer films doped with compound 4d

The preparation of the polymethylmethacrylate (PMMA) film was performed by dissolving the PMMA powder (0.1 g) in chloroform, followed by addition of porphyrinic ligand **4d** (0.001-0.005 g) dissolved in the same solvent. The polymer films were obtained after solvent evaporation at 40 ºC under vacuum for 24 h.[50,51] Due to the spectroscopic characteristics the films doped with 0.005 g of compound **4d** were selected for the studies with the metal ions.

RESULTS AND DISCUSSION

Synthesis

In our first studies concerning the condensation of 2-formyl-5,10,15,20-tetraphenylporphyrin **3** with different aryl methyl ketones[30] we verified, as it was mentioned above, that the use of ammonium acetate is responsible for the formation of porphyrin-2-ylpyridines **1**. So, based on our goal to obtain the corresponding porphyrin-chalcone type derivative as the major compound we decided to re-examine the use of piperidine as base described by Ishkov and co-workers in Claisen-Schmidt condensations involving 2-formyl-porphyrins and ketones.[52,53]

These authors highlighted that the formation of the desired condensation products in appreciable amounts only occurs with the addition of a few drops of perchloric acid.[52] In order to avoid the hazards associated with the use of that acid and knowing that $La(OTf)_3$ is an excellent Lewis acid[54] even in the presence of water we decided to test this reagent in those condensations (Scheme 1).

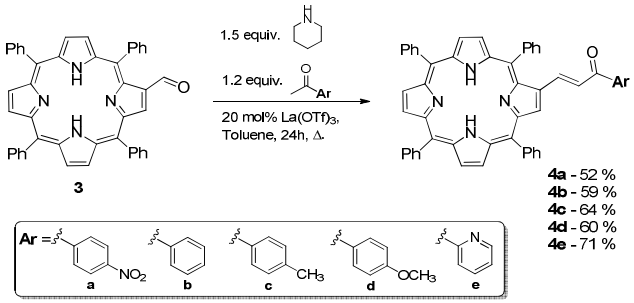

Scheme 1 Synthetic route for compounds **4a-e**.

In a typical experiment, a toluene solution of porphyrin **3**, the aryl methyl ketone (1.2 equiv.), piperidine, (1.5 equiv.) and $La(OTf)_3$ (20 mol%) was heated at reflux for 24 h. A TLC of the reaction mixture revealed the total consumption of starting porphyrin **3** and the formation of chalcone type derivative **4** as the major product (yields between 52% and 71%) accompanied by minor amounts of the corresponding benzoporphyrin **1** (between 1% and 3%).

The compounds were easily purified by silica gel column chromatography and their structures were unambiguously confirmed by NMR and FTIR (Figure 1_SM to Figure 17_SM in ESI), UV-Vis (Figure 18_SM in ESI), and MALDI-TOF mass spectroscopy (Figure 31_SM, Figure 42_SM and Figure 53_SM in ESI). In particular, the ^{1}H NMR spectra of compounds **4a-e** show characteristic peaks in the aromatic region, namely a singlet at *ca.* 9 ppm corresponding to the resonance of the β-pyrrolic proton H-3 and an AB system signal at *ca*. 7.5 ppm due to the resonance of the two protons from the α,β-unsaturated ketone moiety; a coupling constant of ~15 Hz confirms the *trans* configuration of the exocyclic double bond.[55] The ^{13}C NMR spectra show a distinctive signal at *ca*. 190.0 ppm corresponding to the carbonyl carbon (see ESI).

Photophysical Properties

The photophysical characterization of compounds **4a-e** was performed in chloroform solution at 298 K and the main photophysical data are reported in Table 1. In Figure 2 is shown the absorption, excitation and emission spectra of compound **4c** as an example of this porphyrin-chalcone type series. In the same figure is also shown the emission spectrum obtained for the same derivative in the solid state.

The absorption spectra of porphyrin-chalcone type derivatives **4a-e** show the typical features of free base porphyrins due to π–π* transitions (Figure 18_SM in ESI). The representative absorption spectra show highly intense Soret band at *ca*. 435 nm and well-defined four Q bands with decrease intensity between 525 and 661 nm. The perfect match between the absorption and the excitation spectra rules out the presence of any emissive impurity.

The fluorescence emission spectra of compounds **4a-e** obtained after excitation at *ca*. 600 nm present two bands centered at *ca*. 671 and 728 nm, that are characteristic of porphyrins derivatives (Figure 2 for compound **4c**, Figure 18_SM in ESI for compounds **4a**, **4b**, **4d** and **4e**). In all cases it is observed that the first vibrational mode of the fluorescence is more pronounced. The porphyrin-chalcone type derivatives **4a-e** showed Stokes shifts around 10 nm (Table 1).

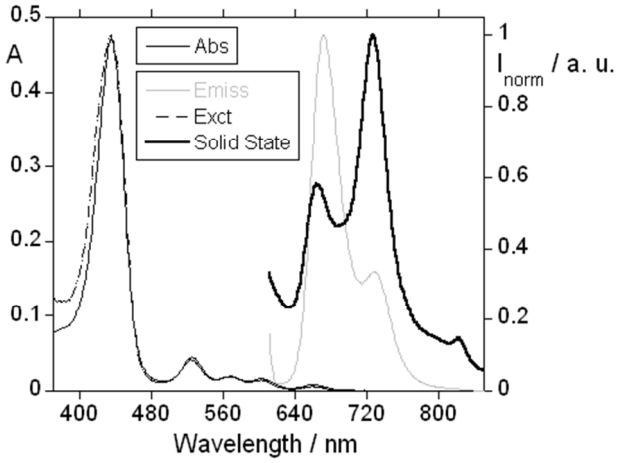

Fig. 2 Absorption and normalized emission and excitation of probe **4c** in $CHCl_3$ ([**4c**] = 2.50 x 10^{-6} M, λ_{exc4c} = 601 nm and $\lambda_{emiss4c}$ = 728 nm) and emission spectra in solid state at room temperature.

Table 1 Photophysical data of compounds **4a-e** in $CHCl_3$ and in solid state at 298 K.

Comp.	λ_{max}(nm) : log ε	λ_{em} (nm)	Stokes Shift (nm)	Φ_{Flu}	λ_{em} (nm)$_{solid}$
4a	435 : 5.05 527 : 4.07 571 : 3.62 602 : 3.61 663 : 3.30	676, 728	13	0.02	679, 766, 821
4b	433 : 5.29 524 : 4.24 562 : 3.84 599 : 3.78 659 : 3.52	669, 728	10	0.02	681, 741,821
4c	435 : 5.22 525 : 4.22 568 : 3.84 601 : 3.78 661 : 3.52	671, 728	10	0.02	664, 727, 823
4d	434 : 5.20 525 : 4.19 567 : 3.83 601 : 3.74 660 : 3.45	671, 727	11	0.03	684, 735, 821
4e	438 : 5.05 526 : 4.15 573 : 3.83 603 : 3.74 662 : 3.44	673, 731	11	0.03	697, 751, 822

The fluorescence quantum yields (Φ_{Flu}), determined by the internal reference method with respect to a solution of crystal violet in methanol as a standard ([Φ] = 0.54),[48,49] are shown in Table 1. Compounds **4a-e** presented lower relative fluorescence quantum yields (0.02 and 0.03) than related free base porphyrins (Φ_{Flu} of TPP = 0.11). The low fluorescence efficiency of this type of molecules can probably be attributed to an alteration of the planarity of the porphyrin core, due to the presence of the extra chain that can be responsible by a more reduced π -electron mobility.[56]

The emission spectra of the solid powder of ligands **4a-e** were also measured, using a fiber optic system connected to the Horiba Jobin-Yvon Fluoromax 4 (Table 1, Figure 2 for compound **4c** and Figure 18_SM in ESI for compounds **4a**, **4b**, **4d** and **4e**). These solid-state spectra show fluorescence bands between 664-823 nm with maximum intensities different to the ones observed in solution.

Spectrophotometric and Spectrofluorimetric Titrations and Metal-Sensing Effects

The sensorial ability of compounds **4a-e** towards the metal ions Zn^{2+}, Cu^{2+}, Hg^{2+}, Cd^{2+} and Ag^{+} and of compound **4d** towards Na^{+}, K^{+}, Tl^{+}, Ca^{2+}, Mg^{2+}, Mn^{2+}, Co^{2+}, Ni^{2+}, Pb^{2+}, Fe^{2+}, Fe^{3+}, Cr^{3+} and $Al^{3+}$was investigated by titrating the ligands, dissolved in chloroform, with small amounts of the adequate metal salt dissolved in acetonitrile**.** These experiments were followed by UV/Vis and fluorescence emission spectroscopy and were performed at 25 ºC.

Zn^{2+} metal ion titration

The addition of aliquots of $(Zn(BF_4)_2.xH_2O)$ in acetonitrile to a solution of porphyrin-chalcone type derivatives **4a-e** in $CHCl_3$ promoted significant changes in the ground and excited state (Figure 3 for compound **4d** and Figure 19_SM in ESI for compounds **4a**, **4b**, **4c** and **4e**). In all cases were observed a red shift (*ca.* 10-15 nm) of the initial *Soret* band probably due to the interaction of Zn^{2+} with the electron lone-pair of the inner N atoms of the porphyrin macrocycle. For compounds **4b**, **4c** and **4d**, well-defined isosbestic points were observed at *ca.* 442 nm, suggesting the presence of two species in solution, which are the free molecular probe and the mononuclear metal complex.

Considering the Q band region the alterations were dependent on the derivative; for compounds **4a**, **4b** and **4e**, the addition of Zn^{2+} induced a decrease in the absorption band centered *ca.* 525 nm with the concomitant increase in the intensity of the remaining three Q bands accompanied by a bathochromic shift of ≈15 and ≈10 nm for the bands centered at *ca.* 600 and 665 nm, respectively (Figure 19_SM in ESI). For compounds **4c** and **4d**, in the first part of the titration the behaviour has similar features to the previous description - decrease in the band centered at *ca.* 525 with the concomitant appearance of a new band at *ca.* 675 nm; however in the end of the titration only two Q bands centered at *ca.* 565 and 600 nm were detected. These spectral changes can be attributed in these two derivatives to the coordination of metal to the inner nitrogen atoms of the macrocycle (vide infra the NMR titrations).

The alterations observed in the absorption spectra of compounds **4a-e** after the titration with Zn^{2+} resulted in a colour change from yellowish-brown to green as it is shown in Figure 4 for compound **4d**.

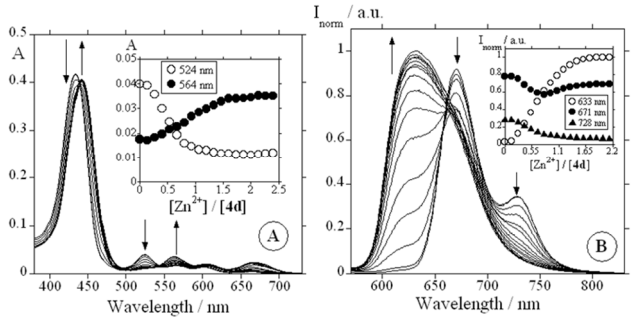

Fig. 3 Spectrophotometric (**A**) and spectrofluorimetric (**B**) titrations of compound **4d** in chloroform as a function of added Zn^{2+} in acetonitrile. The insets show the absorption at 524 and 564 nm (**A**) and the normalized fluorescence intensity at 633, 671 and 728 nm (**B**) ([**4d**] = 2.50 x 10^{-6} M, λ_{exc4d} = 549 nm).

Considering the emission spectra, derivatives **4a-e** showed in general a strong ratiometric response to Zn^{2+} in the excited state (Figure 3 for compound **4d** and Figure 19_SM in ESI for compounds **4a**, **4b**, **4c** and **4e**). As an example, for compound **4d** (Figure 3B), the decrease in the two bands centred at *ca.* 671 and 728 nm, due to the free base porphyrin emission Q (0–0) and Q (0–0)(0–1)[57] is accompanied by the appearance of a new band at *ca.* 633 nm. This new emission band, which increases with the addition of Zn^{2+}, can be assigned to a metal-to-ligand charge transfer and indicates the generation of a new fluorophore arising from the metal-porphyrin association.

The appearance of this blue-shifted emission band leads to a remarkable colour change in the emission from red to intense orange for probes **4a-e** in the presence of Zn^{2+} (Figure 4 for compound **4d**). The remarkable increase in the intensity ratio ($I_{norm(633\ nm)}/I_{norm(671nm)}$) that accompanies the large blue shift in emission upon binding to Zn^{2+} is shown in Figure 20_SM (in ESI) for compound **4d**.

In order to evaluate if the metal counter-ion affects the sensing ability of these compounds, compound **4d,** selected as representative of the series, was titrated with $Zn(NO_3)_3.xH_2O$, $ZnCl_2$ and $Zn(OTf)_2.xH_2O$ in the same conditions described for the previous titrations with $Zn(BF_4)_2.xH_2O$ - the ligand dissolved in chloroform and the addition of the metal carriers in acetonitrile. The alterations observed in the absorption and emission spectra of compounds **4d** (Figure 21_SM and Table 1_SM in ESI) required the addition of 10 equiv. of $Zn(NO_3)_3.xH_2O$ and of 5 equiv. $Zn(OTf)_2.xH_2O$ towards 1 equiv. of $Zn(BF_4)_2.xH_2O$ used. With $Zn(OTf)_2.xH_2O$ the ratiometric response to the metal in the excited state was not so noticeable as it was observed with the two other salts. In the presence of $ZnCl_2$ no changes were observed in the ground and excited state. The results obtained suggest that tetrafluoroborate was the preferential counter-ion to carry out these experiments.

In order to evaluate if the intensity of the emission band at *ca.* 633 nm is affected by the presence of other metals ions, competitive experiments with compound **4d** in the presence of Zn^{2+}, Pb^{2+}, Cd^{2+}, Fe^{3+}, Mg, Al^{3+}, ca^{2+}, Cr^{3+}, Hg^{2+} and Cu^{2+} were performed (Figure 22_SM and Figure 23_SM in ESI). The results show in general a higher affinity and selectivity for Zn^{2+} metal.

The reversibility of the interaction of this series of compounds with Zn^{2+} was also analysed by evaluating the alterations in the UV-VIS and emission spectra of compound **4d** after being titrated with Zn^{2+} in the presence of different amounts of ethylenediaminetetraacetic acid (EDTA) (Figure 24_SM in ESI). The results show that the process is irreversible in the presence of this practical metal catching compound.

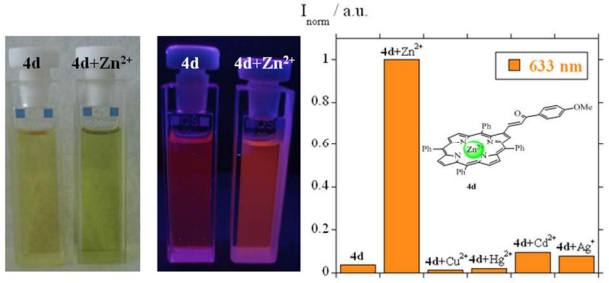

Fig. 4 Physical appearance of a solution of **4d** in chloroform before and after the addition of Zn^{2+} at visible light and after excited at 365 nm using a fluorescence lamp (left). Comparative fluorescence response of probe **4d** (2.50 x 10^{-6} M, λ_{exc4d} = 549 nm) to Zn^{2+}, Cu^{2+}, Hg^{2+}, Cd^{2+} and Ag^{+} (1 equiv.) in chloroform and proposed binding mode of probe **4d** with Zn^{2+} (right).

Cu^{2+} metal ion titration

The titration of compounds **4a-d** with Cu^{2+} ion induced in their ground state a decrease in the *Soret* band centred at *ca.* 433 nm and in the Q bands centred at *ca.* 529 and 670 nm (Figure 5 for compound **4b** and Figure 25_SM in ESI for compounds **4a**, **4c**, **4d**). These alterations are accompanied by the appearance of two bands at *ca.* 555 nm and *ca.* 600 nm that are in agreement with the coordination of the metal in the inner core of the macrocycle. For the porphyrin-chalcone type derivatives **4e** containing a pyridine unit, the Soret band at 438 nm suffers a blue shift to 24 nm; the detection of an isosbestic point at 422 nm suggests the presence of two species in solution, the free probe and the metal complex (Figure 25_SM in ESI). In the Q band region it was only observed an increase in the bands centred at 529 and 670 nm without the disappearance of the bands at 555 nm and 603 nm.

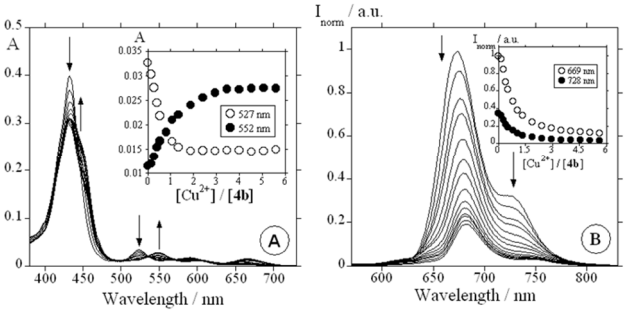

Fig. 5 Spectrophotometric (**A**) and spectrofluorimetric (**B**) titrations of compound **4b** in chloroform as a function of added Cu^{2+} in acetonitrile. The insets show the absorption at 527 and 552 nm (**A**) and the normalized fluorescence intensity at 669 and 728 nm (**B**) ([**4b**] = 2.50 x 10^{-6} M, λ_{exc4b} = 542 nm).

Considering the excited state the addition of Cu^{2+} ion is responsible by a significant decrease in the fluorescence emission of all the derivatives (Figure 5 for compound **4b** and Figure 25_SM in ESI for compounds **4a**, **4c**, **4d, 4d**).[58] This quenching effect, that it is favoured by the presence of the

paramagnetic metal, can be justified considering non-radiative deactivation processes such as: i) reversible electron transfer and ii) formation of the excited triplet state through an electron spin-orbit coupling due to the Cu^{2+} heavy metal effect.[59] So, compounds **4a-e** exhibit fluorescence quenching upon the binding of Cu^{2+} ion typical of "on-off"-type fluoroionophoric probes.

Hg^{2+} and Cd^{2+} metal ion titrations

In the UV-VIS spectra of dyes **4a-e**, the titration with Hg^{2+} is responsible by a red shift in the Soret band from *ca.* 435 nm to 450 nm, probably due to the metal interaction with the electron lone-pair of the inner *N* atoms of the macrocycle. Well-defined isosbestic points were observed at *ca.* 440 nm, suggesting the presence of two species in solution, which are the free ligand and the mononuclear metal complex. The appearance of a new band at *ca*. 666 nm is accompanied by the decrease of the Q bands (Figure 6 for compound **4e** and Figure 26_SM in ESI for compounds **4a-d**).

It is well known that Hg^{2+} ion acts as a fluorescence quencher *via* a spin-orbital coupling effect and therefore, most sensing systems are based on Hg^{2+} turn-off mechanism.[60-64] Compounds **4a-e** showed this behaviour in the excited state, upon titration with the Hg^{2+} where it was possible to observe a significant decrease of the bands at *ca.* 658 nm Q (0–0) and 718 nm Q (0–0)(0–1) as is exemplified for compound **4e** in Figure 6 (Figure 26_SM in ESI for compounds **4a-d**). Similar behaviour was observed after titration of compounds **4a-e** with Cd^{2+}, with a significant quenching of the initial emission bands centred *c.a.* 678 and 728 nm (Figure 27_SM in ESI).

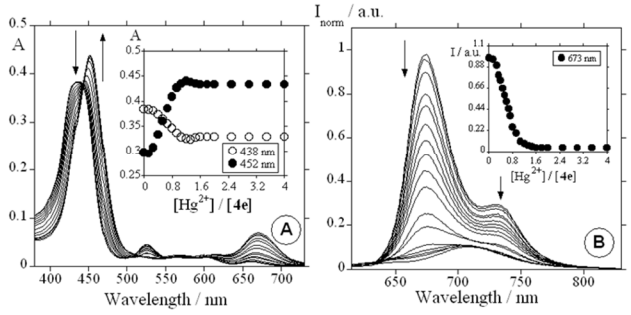

Fig. 6 Spectrophotometric (**A**) and spectrofluorimetric (**B**) titrations of compound **4e** in chloroform as a function of added Hg^{2+} in acetonitrile. The insets show the absorption at 438 and 452 nm (**A**) and the normalized fluorescence intensity at 673 nm (**B**) ([**4e**] = 2.50 x 10^{-6} M, λ_{exc4e} = 545 nm).

Ag^{+} metal ion titrations

Changes in the UV-VIS and emission spectra after titration with Ag^{+} were only observed for dye **4c** In the UV-VIS it was observed a slightly red shift in the Soret band and a decrease of the Q bands band centred at 525 and 661 nm (Figure 7 for compound **4c** and Figure 27_SM in ESI for compounds **4a**, **4b**, **4d**, **4e**).

The emission spectra of compound **4c** upon titration with Ag^{+} showed similar alterations to the ones involving the porphyrin-chalcone type derivatives **4a-e** and Zn^{2+} (Figure 3 for compound **4d** and Figure 19_SM in ESI for compounds **4a**, **4b**, **4c** and **4e**): the decrease in the two bands centred at 671 and 728 nm, due to the free base porphyrin emission Q (0–0) and Q (0–0)(0–1) is accompanied by the appearance of a new band blue-shifted emission band at *ca.* 635 nm. This new emission band, which increases with the addition of Ag^{+}, can be assigned to a metal-to-ligand charge transfer and indicates the generation of a new fluorophore arising from the metal-porphyrin association.

However the small changes observed in the UV-VIS spectra seems to suggest that the coordination does not occur within the porphyrin but on its periphery, namely, in the α,β-unsaturated extra chain. The preferential binding of Ag^{+} metal ion to double bounds has been reported in the literature. Indeed, this type of interaction is being increasingly studied in coordination and supramolecular chemistry.[65,66] In our studies, probably only **4c** due to the moderate electronic-donating features of the methyl group in the phenyl group has the adequate electronic features to favour the interaction with Ag^{+}.

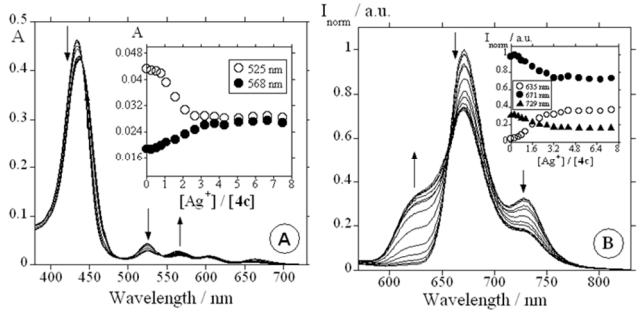

Fig. 7 Spectrophotometric (**A**) and spectrofluorimetric (**B**) titrations of compound **4c** in chloroform as a function of added Ag^{+} in acetonitrile. The insets show the absorption at 525 and 568 nm (**A**) and the normalized fluorescence intensity at 635 and 729 nm (**B**) ([**4c**] = 2.50 x 10^{-6} M, λ_{exc4c} = 545 nm).

Other metal ion titrations

The sensorial ability of compound **4d** was also investigated by UV-VIS and emission spectra in the presence of others mono-, di- and trivalent metal ions such as Na^{+}, K^{+}, Tl^{+}, Ca^{2+}, Mg^{2+}, Mn^{2+}, Co^{2+}, Ni^{2+}, Pb^{2+}, Fe^{2+}, Fe^{3+}, Cr^{3+} and Al^{3+}. No changes were observed when compound **4d** was titrated with the monovalent metal ions and with the divalent ions Mn^{2+}, Co^{2+}, Ni^{2+} and Fe^{2+}. Titrations with Ca^{2+}, Mg^{2+}, Pb^{2+}, Fe^{3+}, Cr^{3+} and Al^{3+} lead to alterations in the UV-VIS and emission spectra similar to the ones previously described for compounds **4a-e** in the presence of Hg^{2+} and Cd^{2+} (see Figure 29_SM).

The stability constants for the interaction of **4a-e** with Zn^{2+}, Cu^{2+}, Hg^{2+} and Cd^{2+}, **4c** with Ag^{+} (Table 2) and **4d** with Ca^{2+}, Mg^{2+}, Pb^{2+}, Fe^{3+}, Cr^{3+} and Al^{3+} (Table 1_SM in ESI) were calculated using HypSpec software.[67] All data is in accordance with a stoichiometry 1:1 ligand-to-metal, which was confirmed by Job's plot method (Figure 30_SM in ESI).

Taking into account the stability constant values the strongest interactions are in general observed between of compounds **4a-e** and Hg^{2+} and Zn^{2+}; this feature permits a mercury and zinc speciation as a function of the absorption and fluorescent signal and of the magnitude of the stability constants.

Table 2. Stability constants for chemosensors **4a-e** in the presence of Zn^{2+}, Cu^{2+}, Hg^{2+}, Cd^{2+} and Ag^{+} in $CHCl_3$ for an interaction 1:1 (metal:ligand).

Compound	Interaction (M:L)	Σ log β (Abs)	Σ log β (Emiss)
4a	Zn^{2+} (1:1)	$6.29 \pm 1.42x10^{-3}$	$6.39 \pm 1.32x10^{-2}$
	Cu^{2+} (1:1)	$6.00 \pm 1.02x10^{-3}$	$6.15 \pm 8.47x10^{-3}$
	Hg^{2+} (1:1)	$8.28 \pm 1.53x10^{-3}$	$8.01 \pm 8.71x10^{-3}$
	Cd^{2+} (1:1)	$6.04 \pm 1.51x10^{-3}$	$5.93 \pm 2.56x10^{-2}$
4b	Zn^{2+} (1:1)	$7.81 \pm 2.39x10^{-3}$	$7.89 \pm 1.28x10^{-3}$
	Cu^{2+} (1:1)	$6.15 \pm 9.05x10^{-4}$	$6.25 \pm 2.81x10^{-2}$
	Hg^{2+} (1:1)	$7.05 \pm 2.55x10^{-3}$	$7.60 \pm 2.53x10^{-2}$
	Cd^{2+} (1:1)	$6.25 \pm 3.78x10^{-2}$	$6.03 \pm 1.25x10^{-2}$
4c	Zn^{2+} (1:1)	$7.40 \pm 2.24x10^{-4}$	$7.92 \pm 1.23x10^{-2}$
	Cu^{2+} (1:1)	$5.70 \pm 1.42x10^{-3}$	$5.37 \pm 1.99x10^{-2}$
	Hg^{2+} (1:1)	$7.39 \pm 2.24x10^{-4}$	$8.18 \pm 2.45x10^{-2}$
	Cd^{2+} (1:1)	$5.86 \pm 1.47x10^{-3}$	$5.58 \pm 1.60x10^{-2}$
	Ag^{+} (1:1)	$6.17 \pm 2.33x10^{-3}$	$5.59 \pm 1.27x10^{-2}$
4d	Zn^{2+} (1:1)	$7.42 \pm 4.25x10^{-3}$	$7.40 \pm 2.33x10^{-2}$
	Cu^{2+} (1:1)	$6.11 \pm 1.70x10^{-3}$	$6.49 \pm 7.87x10^{-3}$
	Hg^{2+} (1:1)	$5.81 \pm 5.81x10^{-3}$	$6.02 \pm 6.67x10^{-2}$
	Cd^{2+} (1:1)	$5.63 \pm 1.21x10^{-3}$	$5.67 \pm 2.41x10^{-2}$
4e	Zn^{2+} (1:1)	$6.84 \pm 2.32x10^{-3}$	$7.09 \pm 1.45x10^{-2}$
	Cu^{2+} (1:1)	$5.65 \pm 1.69x10^{-3}$	$6.18 \pm 7.06x10^{-3}$
	Hg^{2+} (1:1)	$6.62 \pm 1.21x10^{-3}$	$6.66 \pm 6.05x10^{-3}$
	Cd^{2+} (1:1)	$6.12 \pm 1.34x10^{-3}$	$5.83 \pm 9.21x10^{-3}$

Except for silver, the titrations with all the other metals showed spectral evidences suggesting the involvement of the porphyrin inner core in the coordination This is particularly relevant in the titrations with compound **4e** due to the presence of the pyridine unit. Since the metal is only coordinated through two donor–acceptor bonds any interaction with the pyridine unit if weak is probably substituted by interactions with solvent molecules, leading to the dissociation of the complex.

However, the presence of the extra chain in the porphyrin core seems fundamental to improve the sensorial ability of these series of porphyrins. In fact, the absorption and emission spectra obtained after the titration of the non-substituted synthetic precursor 5,10,15,20-tetraphenylporphyrin (TPP) with Hg^{2+}, Cu^{2+}, Zn^{2+}, Cd^{2+} and Ag^{+} (data not shown) did not show significant changes when the same amount of the metal ion was added. The addition of a large amount of the metal ions (*ca.* 10 equiv.) is required to observe changes in the ground and excited states of TPP and the stability constants obtained for those interactions are lower than the ones determined for compounds **4a-e** (Table 2). Taking into account these values, the sequence of the strongest interaction obtained for TPP decreases in the follow order: $Hg^{2} > Cd^{2+} > Zn^{2+} > Cu^{2+} > Ag^{+}$.

Having in mind the use of probes **4a-e** for real metal-ion detection in analytical applications, their limits of detection (LOD) and quantification (LOQ) were determined for Zn^{2+}, Cu^{2+}, Hg^{2+}, Cd^{2+} and Ag^{+}. For these measurements, ten different analyses for each receptor were performed to obtain the LOQ, and a calibration fit was applied to determine the LOD (see experimental part). The values (in ppm) obtained under our experimental conditions are compiled in Table 2_SM in ESI. The LOD and LOQ values show that the best candidates for the detection of Zn^{2+}, Hg^{2+} and Cd^{2+} were respectively compounds **4b**, **4a** and **4e** being the minimum amounts detectable 80, 60 and 140 ppb. In addition, compounds **4b-e** are able to detect a minimum amount of 70 ppb of Cu^{2+} and **4c** 380 ppb of Ag^{+}.

Spectrophotometric and Spectrofluorimetric Studies Using Solid Support Probes

Considering the possibility of using porphyrin-chalcone type derivatives **4a-e** as real molecular probes, low cost polymers based on polymethylmethacrylate (PMMA) were prepared in the absence of water. For these experiments, compound **4d** was selected as representative example. This strategy is very simple and is commonly applied for emissive lanthanide complexes that increase the luminescence and brightness in the absence of water.[68-72]

Figure 8 shows the emission spectra obtained with the PMMA film doped with compound **4d** at room temperature (25 ºC) and although with less defined bands than the ones obtained in solution and solid state (Figure 18_SM in ESI) its similitude with the solid state spectrum is patent in terms of the relative intensity of the bands. The emission behaviour of the PMMA film doped with compound **4d** was also studied after keeping the polymer for two hours at - 20 ºC and 50 ºC. The obtained spectra show in both cases an enhancement in the fluorescence emission (Figure 8A).

In this context, and considering the results in solution, polymers doped with compound **4d** were immersed in an aqueous solution containing Hg^{2+} (1.00×10^{-3} M) or Zn^{2+} (1.00×10^{-3} M). After that, the emission spectra of the doped polymers were registered at different temperatures using an optical fiber device connected to the spectrofluorimeter.

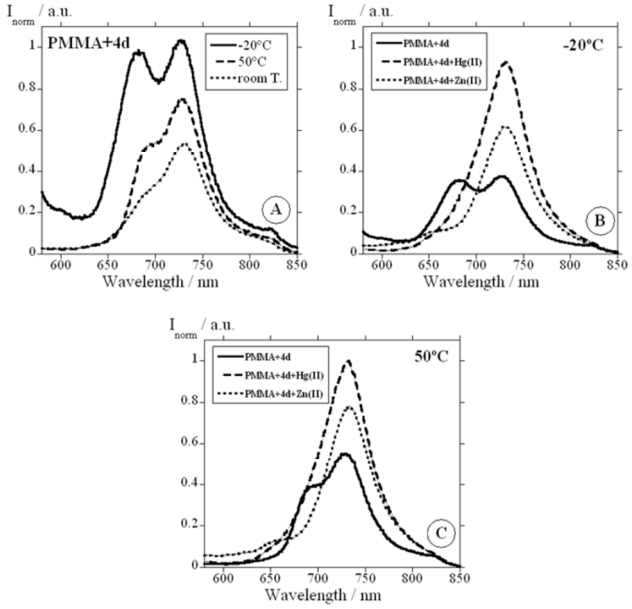

Fig. 8 Emission spectra in solid state of PMMA film doped with **4d** at room temperature, -20 ºC and 50 ºC (**A**). Emission spectra of the PMMA doped film with compound **4d** after spraying with Zn^{2+} or Hg^{2+} at room temperature (**B**) -20 ºC (**C**) and 50ºC; λ_{exc4d} =546 nm.

As it is shown in Figure 9, the interaction of the PMMA films doped with compound **4d** with the ions Hg^{2+} or Zn^{2+} at room temperature is confirmed by the colour change from dark to light brown and also by the enhancement in the fluorescence emission of these films.

The results showed that at -20ºC (Figure 8B) and 50 ºC (Figure 8C) an enhancement in the fluorescence emission was observed in the presence of Zn^{2+} and Hg^{2+} similar to that observed at room temperature (Figure 9).

The relative intensity of the emission bands was an useful tool to discern between Hg^{2+} and Zn^{2+} metal ions, being higher in the presence of Hg^{2+} in all the range of temperatures tested (-20 ºC, 25 ºC and 50 ºC).

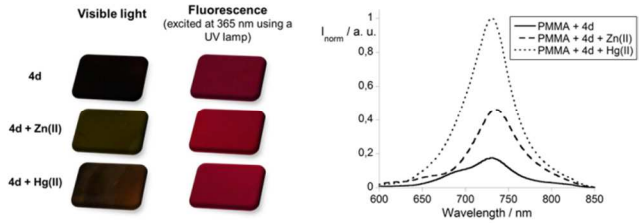

Fig. 9 Visual changes and increase on the emission when PMMA film with the molecular probe **4d** was immersed in an aqueous solution containing Hg^{2+} (1.00 x 10^{-3} M) or Zn^{2+}(1.00 x 10^{-3} M) at room temperature (25 ºC).

These preliminary results show clearly a promising application of compound **4d** in PMMA polymer as new solid supported metal probe of Zn^{2+} and Hg^{2+} in solid phase namely at the studied temperature range.

NMR titrations

In order to investigate the different reaction pathways of **4a-e** with Zn^{2+}, the addition of this metal ion was monitored by ^{1}H NMR. These controls were performed by adding the metal ion in CD_3CN to a solution of the corresponding molecular probe (**4a** and **4c** as examples of the two different situations concerning the UV-Vis titrations) in $CDCl_3$.

The interaction of compound **4a** with Zn^{2+} was corroboratively evidenced also by ^{1}H NMR spectra titration as it is shown in Figure 10. The *N*H protons inside the porphyrinic macrocycle, that appear as a singlet at -2.5 ppm are still present after the titration but as two pairs of separate singlets. These results can be justified by the presence of two tautomers due to the loss of symmetry induced by the presence of the α,β-unsaturated system on position 2 of the porphyrinic macrocycle and consequently the N*H* are not equivalents.[73]

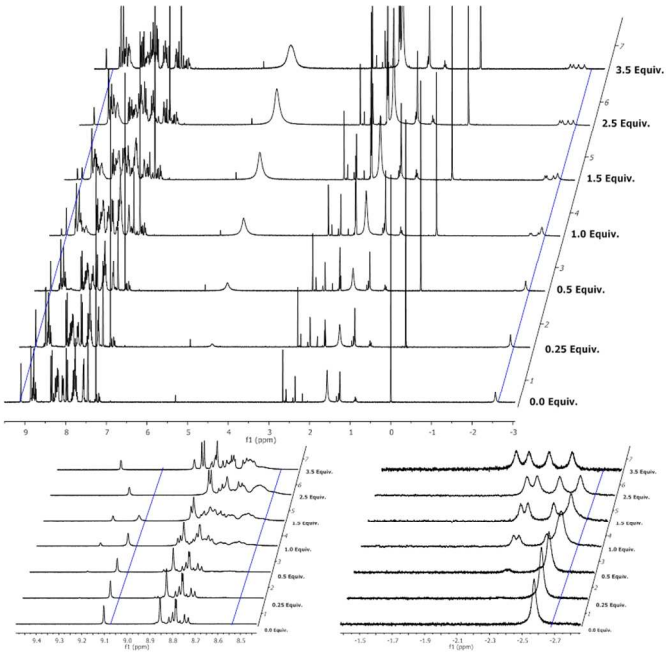

Fig. 10 ^{1}H NMR spectra of **4a** (2.5 x 10^{-3} mM) in $CDCl_3$ upon addition of increasing amounts of Zn^{2+} (from 0 to 3.5 equiv.) in CD_3CN.

A different behaviour was observed in the ^{1}H NMR spectra of compounds **4c** (Figure 30_SM) at the end of the titration with Zn^{2+}. In this case, the disappearance of the signal at -2.5 ppm assigned to the internal N-*H* protons show in the beginning of the titration the presence of the two tautomers that suffers an evolution to a deprotonated form. This behaviour is in accordance with the formation of the metal complex in the absorption spectra with the appearance of only two Q bands centred at *ca.* 565 and 600 nm.

So, based on the alterations of the UV-Vis spectra, we can conclude that compounds **4c** and **4d** loosed the internal N-H protons upon titration with Zn^{2+}, while in the interaction of the other derivatives **4a**, **4b** and **4e** the inner protons are maintained. Probably the contribution in **4c** and **4d** of more stable resonance structures due to the presence of the electron-donating methyl and methoxy groups facilitate the elimination of the internal N-H protons after the coordination of the metal.

Spectrometric studies by MALDI-TOF mass spectrometry

The possibility of using the porphyrin-chalcone type compounds as molecular probes of Zn^{2+}, Cu^{2+}, Hg^{2+}, Cd^{2+} and Ag^{+} ions in the gas phase was also evaluated by MALDI-TOF-MS with ligands **4b** (Figure 31_SM to Figure 41_SM in ESI), **4d** (and Figure 42_SM to Figure 52_SM in ESI) and **4e** (Figure 53_SM to Figure 63_SM in ESI). In these experiments the selected ligands **4b**, **4d** and **4e** after being dissolved in chloroform were titrated with the metal salts in acetonitrile using the *"dried-droplet"* approach and the *"layer-by-layer"* deposition (see experimental part). The results obtained with the different metals are summarized in Table 3_SM in ESI (compound **4b**), Table 4_SM (compound **4d**) and Table 3 (compound **4e**). In all cases, with both methods the porphyrin-chalcone type probe acts as an internal matrix.

As an example, Figure 54_SM shows the MALDI-TOF-MS

titration of molecular probe **4e** with $Zn(BF_4)_2.xH_2O$. Before adding the metal salt, the peak corresponding to the molecular probe appears at *m/z* 746.08, with 100% of intensity, can be unambiguously attributed to the species $[\mathbf{4e}+H]^+$ formed in gas phase. After adding 1 equivalent of Zn^{2+}, a peak at *m/z* 806.98 (49% of intensity) was attributed to the species $[(\mathbf{4e}\text{-}3H)+Zn]^{+\bullet}$. With this ligand, the addition of increased amounts of the different metal ions only produced peaks attributable to the formation of dinuclear complexes in the case of Cu^{2+} (Figure 56_SM in ESI). The *"layer-by-layer"* deposition approach showed to be more efficient in the detection of Hg^{2+} and Cd^{2+} (Figure 60_SM and Figure 62_SM in ESI, respectively).

Conclusions

The most significant changes in the ground and excited state were observed for porphyrin-chalcone type derivatives **4a-e** in the presence of Zn^{2+}, Cu^{2+}, Hg^{2+}, Cd^{2+} and **4d** with Ca^{2+}, Mg^{2+}, Pb^{2+}, Fe^{3+}, Cr^{3+} and Al^3 metal ions. Changes in the presence of Ag^+ were only observed for compound **4c**. These results indicated a ligand-to-metal complex stoichiometry of 1:1 as it was confirmed by Job's plot method.

The alterations observed in the absorption and emission spectra of compounds **4a-e** upon titration with Zn^{2+}, namely a colour change of the solution from yellowish-brown to green and the appearance of a blue-shifted emission band that leads to a remarkable colour change in the emission from red to intense orange are important and promising results. These data can be analytically explored to develop a new type of Zn^{2+} ratiometric molecular device, as it can be concluded from the comparative response of probes **4a-e** for Hg^{2+}, Cd^{2+}, Cu^{2+} and Ag^+. In particular, compound **4b** was considered the best candidate to detect this metal being able to quantify 80 ppb of Zn^{2+}.

Preliminary results show clearly a promising application of compound **4d** in PMMA polymer as new solid supported metal molecular probe of Zn^{2+} and Hg^{2+} in solid phase. The results showed that at -20 ºC and 50 ºC an enhancement in the fluorescence emission was observed in the presence of Zn^{2+} and Hg^{2+} similar to that observed at room temperature. This method offered the advantage of the differentiation between both metal ions by monitoring the intensity of the emission bands.

Additionally, the results obtained by MALDI-TOF-MS confirm the gas phase sensing abilities of compounds **4a-e** towards Zn^{2+}, Cu^{2+}, Hg^{2+}, Cd^{2+} and Ag^+.

Table 3 Major peaks observed in the metal titration of probe **4e** followed by MALDI-TOF-MS.

Metal	Stoichiometry (ligand:metal)	Dried-droplet		Layer-by-Layer	
		m/z	Relative intensity (%)	*m/z*	Relative intensity (%)
Zn^{2+}	1:1	746.08	100.00 $[\mathbf{4e}+H]^+$	746.07	100.00 $[\mathbf{4e}+H]^+$
		806.98	49.00 $[(\mathbf{4e}\text{-}3H)+Zn]^{+\bullet}$	806.98	37.12 $[(\mathbf{4e}\text{-}3H)+Zn]^{+\bullet}$
	1:2	746.08	100.00 $[\mathbf{4e}+H]^+$		
		806.98	42.00 $[(\mathbf{4e}\text{-}3H)+Zn]^{+\bullet}$		
Hg^{2+}	1:1	746.08	100.00 $[\mathbf{4e}+H]^+$	745.10	100.00 $[\mathbf{4e}]^{+\bullet}$
	1:2	746.08	100.00 $[\mathbf{4e}+H]^+$	945.06	46.00 $[(\mathbf{4e}\text{-}2H)+Hg]^{+\bullet}$
Cu^{2+}	1:1	746.11	42.00 $[\mathbf{4e}+H]^+$	745.10	9.60 $[\mathbf{4e}]^{+\bullet}$
		806.00	100.00 $[(\mathbf{4e}\text{-}2H)+Cu]^{+\bullet}$	806.01	100.00 $[(\mathbf{4e}\text{-}2H)+Cu]^{+\bullet}$
	1:2	869.35	30.97 $[(\mathbf{4e}\text{-}2H)+2Cu]^{+\bullet}$		
		806.00	100.00 $[(\mathbf{4e}\text{-}2H)+Cu]^{+\bullet}$		
Cd^{2+}	1:1	746.21	100.00 $[\mathbf{4e}+H]^+$	746.10	100.00 $[\mathbf{4e}+H]^+$
	1:2	746.21	100.00 $[\mathbf{4e}+H]^+$	857.00	11.00 $[(\mathbf{4e}\text{-}2H)+Cd]^{+\bullet}$
Ag^+	1:1	746.11	71.00 $[\mathbf{4e}+H]^+$	746.07	17.00 $[\mathbf{4e}+H]^+$
		851.96	100.00 $[(\mathbf{4e}\text{-}H)+Ag]^{+\bullet}$	851.62	100.00 $[(\mathbf{4e}\text{-}H)+Ag]^{+\bullet}$
	1:2	746.06	18.00 $[\mathbf{4e}+H]^+$		
		851.90	100.00 $[(\mathbf{4e}\text{-}H)+Ag]^{+\bullet}$		

Acknowledgements

Authors are grateful to the Universidade de Aveiro, Fundação para a Ciência e a Tecnologia (FCT) European Union, QREN, FEDER and COMPETE for funding the QOPNA research unit (project PEst-C/QUI/UI0062/2013). We acknowledge the Portuguese National NMR Network (RN-RMN), supported by funds from FCT and REQUIMTE (PESt-C/EQB/La0006/2013) for general funding.

Thanks are also due to Scientific PROTEOMASS Association (Portugal) for financial support. N. Moura thanks FCT/MEC for their Post-Doctoral grants SFRH/BPD/84216/2012. C. Núñez thanks Xunta de Galicia for her Postdoctoral Research contract (I2C Program).

We thank Sérgio M. Santos for the helpful comments and discussion concerning the interactions with silver ions.

Notes and references

[a] *Chemistry Department and QOPNA, University of Aveiro, Campus Universitário Santiago, 3810-193 Aveiro, Portugal. Tel: +351 21 2948300; E-mail: gneves@ua.pt*

[b] *BIOSCOPE Group, REQUIMTE-CQFB, Chemistry Department, Faculty of Science and Technology, University NOVA of Lisbon, 2829-516 Monte de Caparica, Portugal. Fax: +351 21 2948550; Tel: +351 21 2948300 ;E-mail: cle@fct.unl.pt*

[c] *ProteoMass Scientific Society. Madan Parque. Rua dos Inventores. 2825-182. Caparica. Portugal.*

[d] *Ecology Research Group, Department of Geographical and Life Sciences, Canterbury Christ Church University, CT1 1QU Canterbury, United Kingdom.* cristina.nunez@fct.unl.pt
[e] *Inorganic Chemistry Department, Faculty of Chemistry, University of Santiago de Compostela, 15782 Santiago de Compostela, Spain*

† Electronic Supplementary Information (ESI) available: [details of any supplementary information available should be included here]. See DOI: 10.1039/b000000x/

1 Y. Jeong and J. Yoon, *Inorg. Chim. Acta*, 2012, **381**, 2.
2 M. Formica, V. Fusi, L. Giorgi and M. Micheloni, *Coord. Chem. Rev.*, 2012, **256**, 170.
3 C. Kar, M. D. Adhikari, A. Ramesh and G. Das, *Inorg. Chem.*, 2013, **52**, 743.
4 M. Pamuk and F. Algi, *Tetrahedron Lett.*, 2012, **53**, 7117.
5 W. Wang, Q. Wen, Y. Zhang, X. Fei, Y. Li, Q. Yang, X. Xu, *Dalton Trans.*, 2013, **42**, 1827.
6 M. Pamuk and Fatih Algi, *Tetrahedron Lett.*, 2012, **53**, 7010.
7 J.-M. An, M.-H. Yan, Z.-Y. Yang, T.-R. Li, Q.-X. Zhou, *Dyes and Pigments*, 2013, **99**, 1.
8 S. Atilgan, T. Ozdemir and E. U. Akkaya, *Org. Lett.*, 2010, **12**, 4792.
9 N. Kaur and S. Kumar, *Tetrahedron*, **2011**, **67**, 9233.
10 J. S. Kim and D. T. Quang, *Chem. Rev.*, 2007, **107**, 3780.
11 L.-J. Fan, Y. Zhang, C. B. Murphy, S. E. Angell, M. F. L. Parker, B. R. Flynn and W. E. Jones Jr., *Coord. Chem. Rev.*, 2009, **253**, 410.
12 L. N. Neupane, J.-Y. Park, J. H. Park and K.-H. Lee, *Org. Lett.*, 2013, **15**, 254.
13 E. Kimura and T.Koike, *Chem. Soc. Rev.*,1998, **27**, 179.
14 Y.-Q. Weng, F. Yue, Y.-R. Zhong and B.-H. Ye, *Inorg. Chem.*, 2007, **46**, 7749.
15 C.-Y. Li, X.-B. Zhang, Y.-Y. Dong, Q.-J. Ma, Z.-X. Han, Y. Zhao, G.-L. Shen and R.-Q. Yu, *Anal. Chim. Acta*, 2008, **616**, 214.
16 W. H. Chan, R. H. Yamg and K. M. Wang, *Anal. Chim. Acta*, 2001, **444**, 261.
17 H.-Y. Luo, J.-H. Jiang, X.-B. Zhang, C.-Y. Li, G.-L. Shen and R.-Q. Yu, *Talanta*, 2007, **72**, 575.
18 Z.-X. Han, H.-Y. Luo, X.-B. Zhang, R.-M. Kong, G.-L. Shen and R.-Q. Yu, *Spectrochim. Acta A*, 2009, **72**, 1084.
19 R. Buntem, A. Intasiri and W. Luengchaichawewn, *J. Colloid Interf. Sci.*, 2010, **347**, 8.
20 H. N. Kim, W. X. Ren, J. S. Kim and J. Yoon, *Chem. Soc. Rev.*, 2012, **41**, 3210.
21 S. Aoki, K. Sakamura, N. Matsuo, Y. Yamada, R. Takasawa, S.-C. Tanuma, M. Shiro, K. Takeda and E. Kimura, *Chem. Eur. J.*, 2006, **12**, 9066.
22 C.-H. Hung, G.-F. Chang, A. Kumar, G.-F. Lin, L.-Y. Luo, W.-M. Ching and E. W.-G.Diau, *Chem. Commun.*, 2008, 978.
23 Z. Xu, J. Yoon and D. R. Spring, *Chem. Soc. Rev.*, 2010, **39**, 1996.
24 Y. Ding, Y. Xie, X. Li, J. P. Hill, W. Zhang and W. Zhu, *Chem. Commun.*, 2011, **47**, 5431.
25 Y. Yang, J. Jiang, G. Shen and R. Yu, *Anal. Chim. Acta*, 2009, **636**, 83.
26 B. Stefane, *Org. Lett.*, 2010, **12**, 2900.
27 S. V.; Pansare and E. K. Paul, *Chem. Eur. J.*, 2011, **17**, 8770.
28 T. Müller, K. Djanashvili, I. W. C. E. Arends, J. A. Peters and U. Hanefeld, *Chem. Commun.*, 2013, **49**, 361.
29 J. A. S. Cavaleiro, A. C. Tomé and M. G. P. M. S.Neves, *Handbook of Porphyrin Science*, K. M. Kadish, K. M. Smith, R. Guilard Eds., World Scientific Publishing Company Co., Singapore, 2010,vol. 2, pp. 193.
30 N. M. M. Moura, M. A. F. Faustino, M. G. P. M. S. Neves, F. A. A. Paz, A. M. S. Silva, A. C. Tomé and J. A. S. Cavaleiro, *Chem. Commun.*, 2012, **47**, 6142.
31 Z. Nowakowska, *Eur. J. Med. Chem.*, 2007, **42**, 125 and references therein.
32 B. P. Bandgar, S. S. Gawande, R. G. Bodade, J. V. Totre and C. N. Khobragade, *Bioorg. Med. Chem.*, 2010, **18**, 1364.
33 A.-M. Katsori and D. Hadjipavlou-Litina, *Expert Opin. Ther. Patents*, 2011, **21**, 1575.
34 A. Kamal, M. K. Reddy and A. Viswanath, *Expert Opin. Drug Discov.*, 2013, 8, 289.
35 K. Rurack, J. L. Bricks, G. Reck, R. Radeglia and U. Resch-Genger, *J. Phys. Chem. A*, 2000, **104**, 3087.
36 L. Mager, C. Melzer, M. Barzoukas, A. Fort, S. Méry and J.-F. Nicoud, *Appl. Phys. Lett.*, 1997, **71**, 2248.
37 Z. K. Si, Q. Zhang, M. Z. Xue, Q. R. Sheng and Y. G. Liu, *Res. Chem. Intermed.*, 2011, **37**, 635.
38 J. Muzart, *Eur. J. Org. Chem.*, 2010, 3779.
39 D. G. Piotrowska, M. Cieslak, K. Królewskaand A. Wróblewski, E. *Eur. J. Med. Chem.*, 2011, **46**, 1382.
40 C. Lodeiro, J. L. Capelo, J. C. Mejuto, E. Oliveira, H. M. Santos, B. Pedras and Núñez, C. *Chem. Soc. Rev.*, 2010, **39**, 2948.
41 C. Lodeiro and F. Pina, *Coord. Chem. Rev.*, 2009, **253**, 1353.
42 M. Galesio, D. V. Vieira, R. Rial-Otero, C. Lodeiro, I. Moura and J. L. Capelo, *J. Proteome Res.*, 2008, **7**, 2097.
43 M. Mameli, V. Lippolis, C. Caltagirone, J. L. Capelo, O. N. Fazaand and C. Lodeiro, *Inorg. Chem.*, 2010, **49**, 8276.
44 C. Núñez, R. Bastida, A. Macías, L. Valencia, J. Ribas, J. L. Capelo and C. Lodeiro, *Dalton Trans.*, 2010, **39**, 7673.
45 H. M. Santos, C. Lodeiro and J. L. Capelo, *J. Proteomics*, 2010, **73**, 1411.
46 W. L. F. Armarego and D. D. Perrin, *Purification of Laboratory Chemicals*, 4th Edt.; Butterworth-Heinemann: Oxford, 1996.
47 N. M. M. Moura, M. A. F. Faustino, M. G. P. M. S. Neves, A. C. Duarte and J. A. S. *J.* Cavaleiro, *Porphyrins Phthalocyanines*, 2012, **15**, 652.
48 I. B. Berlman, *Handbook of Fluorescence Spectra of Aromatic Molecules*, 2nd ed.; Academic Press: New York, 1971.
49 M. Montalti, A. Credi, L. Prodi and M. T. Gandolfi, *Handbook of Photochemistry*, 3rd ed.; Taylor & Francis: Boca Raton, FL, 2006.
50 D. B. A. Raj, B. Francis, M. L. P. Reddy, R. R. Butorac, V. M. Lynch and A. H. Cowley, *Inorg. Chem*., 2010, **49**, 9055.
51 O. Moudam, B. C. Rowan, M. Alamiry, P. Richardson, B. S. Richards, A. C. Jones and N. Robertson, *Chem. Commun.*, 2009, 6649.
52 Y. V. Ishkov, Z. I. Zhilina and L. P. Barday, *J. Porphyrins Phthalocyanines*, 2003, **7**, 761.
53 Y. V. Ishkov, Z. I. Zhilina, L. P. Bardai and S. V. Vodzinskii, *Russian J. Org. Chem.*, 2004, **40**, 434.
54 a) C. Alonso, V. I. V. Serra, M. G. P. M. S. Neves, A. C. Tomé, A. M. S. Silva, F. A. A. Paz and J. A. S. Cavaleiro, *Org. Lett.*, 2007, **9**, 2305. b) C. Alonso, M. G. P. M. S. Neves, A. C. Tomé, A. M. S. Silva and J. A. S. Cavaleiro, *Eur. J. Org. Chem.*, 2004, 3222.
55 a) P. Baas and H. Cerfontain, *Tetrahedron*, 1977, **33**, 1509. b) S. Shibata, *Stem Cells*, 1994, **12**, 44. c) J. B. Lambert and E. P. Mazzola, *Nuclear Magnetic Ressonance Spectroscopy – AnIntrodution to Principles, Applications and Experimental Methods*, Prentice Hall: New Jersey, 2004.
56 *Fundamentals of Photochemistry*, K. K. Rohatgi-Mukherjee, Jadavpu University, Calcutta,Wiley Eastern Limited, **1992**.
57 Z.-X. Han, H.-Y. Luo, X.-B. Zhang, R.-M. Kong, G.-L. Shen and R.-Q. Yu, *Spectrochim. Acta Part A*, 2009, **72**, 1084.
58 M. P. Algi, Z. Öztaş and F. Algi, *Chem. Commun*., 2012, **48**, 10219.
59 J. G. Xu and Z. B. Wang, *Fluorescence Analytic Method*, Science Press, Beijing, 2006, pp. 39 (in Chinese).
60 M.-Y. Chae and A. W.Czarnik, *J. Am. Chem. Soc*., 1992, **114**, 9704.
61 K. Rurack, M. Kollmannsberger, U. ReschGenger and J. Daub, *J. Am. Chem. Soc.*, 2000, **122**, 968.
62 L. Prodi, C. Bargossi, M. Montalti, N. Zaccheroni, N. Su, J. S. Bradshow, R. M. Izatt and P. B. Savage, *J. Am. Chem. Soc.*, 2000, **122**, 6769.
63 S.-Y. Moon, N. R. Cha, Y. H. Kim and S.-K. Chang, *J. Org. Chem.*, 2004, **69**, 181.
64 S.-Y. Moon, N. J. Yoon, S. M. Park and S.-K. Chang, *J. Org. Chem.*, 2005, **70**, 2394.

65 H. Yin and N. A. Porter, *Method. Enzymol.*, 2007, **433**, 193.
66 J. Burgess and P. J. Steel, *Coordin. Chem. Rev.*, 2011, **255**, 2094.
67 P. Gans, A. Sabatini and A.Vacca, *Talanta*, 1996, **43**, 1739.
68 M. D. McGehee, T. Bergstedt, C. Zhang, A. P. Saab, M. B. O'Regan, G. C. Bazan, V. I. Srdanov and A. J. Heeger, *Adv. Mater.*, 1999, **11**, 1349.
69 J. Kai, D. F. Parrab and H. F. Brito, *J. Mater. Chem.*, 2008, **18**, 4549.
70 A. Balamurugan, M. L. P. Reddy and M. Jayakannan, *J. Phys. Chem. B*, 2009, **113**,14128.
71 J. C. Boyer, N. J. J. Johnson and F. C. J. M. van Veggel, *Chem. Mater.*, 2009, **21**, 2010.
72 H. Zhang, H. Song, B. Dong, L. Han, G. Pan, X. Bai, L.Fan, S. Lu, H. Zhao and F. Wang, *J. Phys. Chem. C*, 2008, **112**, 9155.
73 M. J. Crossley, P. L. Burn, S. S. Chew, C. F. Cuttance and I. A. Newsom, *J. Chem. Soc., Chem. Commun*. 1991, 1564.